

Research Article

Emergency Control Scheme Decision with Two-Stage Optimization for HvdC Blocking

Li Huarui^{*} , Zhu Xinyao , Jia Yongyong , Li Zheng , Wang Xiaobo 

State Grid Jiangsu Electric Power Company Limited, Research Institute, Nanjing, China

Abstract

In view of the fact that the existing offline decision making methods cannot meet the requirements for accurate control of the actual operation mode under severe power disturbance events such as DC blocking, a two-stage optimization method of emergency control scheme including pre-optimization and online optimization is proposed by comprehensive application of time domain simulation and machine learning technology. First, typical scenarios reflecting the possible future operation mode of the system are generated in the pre-optimization stage, and multi-resource coordination emergency control schemes in each scenario are optimized by using trajectory sensitivity and machine learning methods, and stored in the knowledge base. In the online optimization stage, the information of the actual operation mode of the system is obtained. Based on metric learning, the appropriate control scheme is selected from the knowledge base as the initial value, and the optimal control scheme under the actual operation mode is obtained by rapid iterative optimization. A multi-dc fed terminal system is taken as an example to verify the effectiveness of the proposed method.

Keywords

New Energy, Multi-Resource Coordination, Emergency Control, Two State Optimization, Frequency Security

1. Introduction

Renewable energy power generation technologies are developed rapidly. The in-stalled capacity and penetration rate of renewable energy in modern power systems are increasing constantly [1]. Renewable energy generation is integrated to power systems with power electronic equipment, which results in decrease of equivalent inertia and increase of frequency fluctuation after power disturbance in power systems [2]. Frequency may drop constantly after power disturbance caused by HVDC (High Voltage Direct Current) transmission blocking, resulting in a large number of loads and units removed, which may lead to instability and collapse of power systems [3]. It's necessary to develop emergency

control scheme decision methods to ensure that the margin requirements of security indicators are satisfied to avoid collapse of power systems.

Emergency load shedding is an important measure to ensure the safety of power systems after large-scale power disturbances, which has been studied in many literatures. In the literature [4], “low-frequency high-voltage” characteristics are made full use of to optimize load-shedding control measures after DC blocking. In the literature [5], transient voltage and frequency safety constraints are comprehensively considered to decide load cutting measures. In the literature [6], the selection method of load cutting point considering

^{*}Corresponding author: lihuarui_sdu@163.com (Li Huarui)

Received: 23 December 2024; **Accepted:** 6 January 2025; **Published:** 17 February 2025



Copyright: © The Author(s), 2025. Published by Science Publishing Group. This is an **Open Access** article, distributed under the terms of the Creative Commons Attribution 4.0 License (<http://creativecommons.org/licenses/by/4.0/>), which permits unrestricted use, distribution and reproduction in any medium, provided the original work is properly cited.

transient power angle stability constraints is proposed. On the basis of emergency load shedding, multi-resource coordination control measures to make full use of available control resources are proposed in some literature. A strategy that comprehensively considering HVDC emergency power modulation and load shedding in Literature [7]. In literature [8], characteristics of different control resources is researched to determine the action sequence of multiple types of resources heuristically. In the literature [9], a coordinated control scheme of DC power modulation and emergency power support considering local and remote information to realize coordinated action among regional power grid systems is proposed. In order to ensure the safety of the receiving end grid with large capacity feed-in DC under severe power disturbance such as DC blocking, it's important to study the coordinated control of multi-resources [10].

There are a large number of possible future operation modes in modern power systems with high proportion of renewable energy penetration. The traditional "offline decision-making, real-time matching" emergency control measure decision-making only take typical operation modes into consideration, resulting that the developed control measures are difficult to satisfy demands for accurate control. [10]. In order to solve the problem that traditional off-line decision-making cannot satisfy the precise control requirements of actual operation mode, some literatures have carried out research on online decision-making of emergency control schemes. In literature [11-13], it's proposed to linearize the relationship between transient safety indicators and control quantity based on trajectory sensitivity method, in order to transform the nonlinear emergency control scheme decision problem into a linear programming problem, which can be solved with the linear programming method. In literature [14], the decision-making problem of emergency control scheme is transformed into a nonlinear programming problem based on dynamic trajectory information of power system, and the step-wise quadratic programming method is used to solve it. In literature [15-17], in order to avoid the problem that emergency control scheme decision methods based on linear or nonlinear programming methods may not converge in some cases, various heuristic algorithms are applied to make emergency control scheme decision, so as to improve the global convergence of the decision process.

In order to improve the accuracy of the control scheme and ensure the decision-making efficiency of the control schemes, the time-domain simulation and machine learning technologies are comprehensively applied in this paper to propose an emergency control scheme optimization method including pre-optimization and online optimization. In the pre-optimization stage, outputs of new energy and loads are predicted to generate typical future scenarios. Optimal control

schemes are obtained based on trajectory sensitivity and machine learning methods, and the schemes are stored into optimization decision knowledge base. In the online optimization stage, the actual operation mode information is obtained, and the appropriate control scheme is selected from the knowledge base as the initial value, for reducing the number of iterations and ensuring decision efficiency. In each optimization iteration, safety indicators are accurately evaluated with time domain simulation to ensure solution accuracy. The effectiveness of the proposed method is verified by an example system.

2. Two-stage Optimization Framework for Emergency Control

2.1. Optimization Model of Multi-resource Coordinated Emergency Control Scheme

The purpose of the multi-resource coordination emergency control scheme optimization is to minimize the control cost F while ensuring that each security indicator satisfies the margin requirements. In this paper, the frequency and voltage security constraints in the form of binary table in the literature [18] are applied, as shown in Eq. (1):

$$\begin{aligned} t(f \leq f_{th,p}) &< t_{th,p}^{fre}, p = 1, \dots, N_{UFLS} \\ t(V_q \leq V_{th}) &< t_{th}^{vol}, q = 1, \dots, N_{ref} \end{aligned} \quad (1)$$

where f denotes the system frequency, $f_{th,p}$ denotes the threshold value of the p th round Under Frequency Load Shedding (UFLS), $t(f \leq f_{th,p})$ denotes the duration time when f is lower than $f_{th,p}$, $t_{th,p}^{fre}$ denotes the time delay of the p th round UFLS, V_q denotes the voltage of the q th reference node after DC blocking, V_{th} denotes the voltage threshold value, $t(V_q \leq V_{th})$ denotes the time when V_q is lower than V_{th} , t_{th}^{vol} denotes the time threshold value related to voltage security indicator, N_{UFLS} and N_{ref} respectively denote the number of rounds of UFLS and reference nodes.

Considering that there are some problems with the traditional binary table method such as poor linearization, this paper refers to the literature [5] to construct the voltage and frequency security indicators as shown in the Eq. (2). Compared with the indicators in the form of the binary table, the cumulative effects are considered with the defined indicators. Meanwhile, the linearity and smoothness of the indicators are better, which is suitable for sensitivity analysis.

$$\begin{aligned}
\eta_p^{\text{fre}} &= \min \left(\frac{\int_{t_0}^{t_{\text{th},p}^{\text{fre}}} (f - f_{\text{th},p}) dt}{(f^N - f_{\text{th},p}) t_{\text{th},p}^{\text{fre}}} \right), 0 \leq t \leq t_{\text{tra}} - t_{\text{th},p}^{\text{fre}} \\
p &= 1, \dots, N_{\text{UFLS}} \\
\eta_q^{\text{vol}} &= \min \left(\frac{\int_{t_0}^{t_{\text{th},q}^{\text{vol}}} (V_q - V_{\text{th}}) dt}{(V_q^N - V_{\text{th}}) t_{\text{th},q}^{\text{vol}}} \right), 0 \leq t \leq t_{\text{tra}} - t_{\text{th},q}^{\text{vol}} \\
q &= 1, \dots, N_{\text{ref}}
\end{aligned} \quad (2)$$

where t denotes the time variable, t_0 denotes the time when the disturbance occurs, η_p^{fre} denotes the p th frequency security indicator obtained based on the frequency-time binary table relevant to UFLS, f^N denotes the rated frequency of the system, η_q^{vol} denotes the voltage security indicator of the q th reference node obtained based on the voltage-time binary table, V_q^N represents the rated voltage of the q th reference node, and t_{tra} is the time duration of the considered transient process.

To ensure that the frequency and voltage indicators satisfy the requirements of the corresponding binary table, it's necessary to ensure that Eq. (3) is satisfied:

$$\begin{aligned}
\eta_p^{\text{fre}} &> \varepsilon_{\text{fre}}, p = 1, \dots, N_{\text{UFLS}} \\
\eta_q^{\text{vol}} &> \varepsilon_{\text{vol}}, q = 1, \dots, N_{\text{ref}}
\end{aligned} \quad (3)$$

where ε_{fre} and ε_{vol} respectively denotes the security indicators margin of frequency and voltage.

The event-driven emergency control is triggered is specifically oriented to specific large-scale power disturbances [19].

In this paper, by solving the optimization problem in Eq. (3) for the foreseen accident, the emergency control scheme under the corresponding foreseen accident is developed. In this paper, by solving the optimization problem in Eq. (4), the emergency control scheme under the corresponding pre-defined contingency is formulated.

$$\begin{aligned}
\min F(P_{\text{els}}, P_{\text{dc}}, P_{\text{ps}}) &= \omega_{\text{els}} \sum_{i=1}^{N_{\text{els}}} P_{\text{els},i} + \omega_{\text{dc}} \sum_{j=1}^{N_{\text{dc}}} P_{\text{dc},j} + \sum_{k=1}^{N_{\text{ps}}} P_{\text{ps},k} \\
\text{s.t. } \quad \eta_p^{\text{fre}} &> \varepsilon_{\text{fre}}, p = 1, \dots, N_{\text{UFLS}} \\
\eta_q^{\text{vol}} &> \varepsilon_{\text{vol}}, q = 1, \dots, N_{\text{ref}} \\
P_{\text{els},i} &\in \{0, P_{\text{els},i}^1, \dots, P_{\text{els},i}^{N_{\text{els},i}}\} \\
0 \leq P_{\text{dc},j} + P_{\text{dc},j}^{\text{ini}} &\leq P_{\text{dc},j}^{\text{max}} \\
P_{\text{ps},k} &\in \{0, P_{\text{ps},k}^1, \dots, P_{\text{ps},k}^{N_{\text{ps},k}}\}
\end{aligned} \quad (4)$$

where ω_{els} and ω_{dc} respectively denote the relative cost weighting coefficients of emergency load shedding and High Voltage Direct Current (HVDC) emergency power modulation relative to pump shedding of pumped storage.

The priority of multi-resource coordinated control is pump shedding of pumped storage, HVDC emergency power modulation and load shedding in descending order. In this paper, ω_{els} and ω_{dc} are taken to be 100 and 10, respectively. $P_{\text{els},i}$, $P_{\text{dc},j}$, and P_{ps} , respectively denotes loads shed of the i th load control substation, emergency power modulated of the j th HVDC, and pump shedding of the k th pumped storage. N_{els} , N_{dc} and N_{ps} respectively denote the number of load control sub-stations, HVDC and pumped storage stations. $P_{\text{els}} = [P_{\text{els},1}, \dots, P_{\text{els},N_{\text{els}}}]$, $P_{\text{dc}} = [P_{\text{dc},1}, \dots, P_{\text{dc},N_{\text{dc}}}]$, $P_{\text{ps}} = [P_{\text{ps},1}, \dots, P_{\text{ps},N_{\text{ps}}}]$. $P_{\text{els},i}^l$ denotes the amount load shedding corresponding to the removal of l feeder lines at the i th load control substation, $N_{\text{els},i}$ denotes the number of feeder lines at the i th load control substation, $P_{\text{dc},j}^{\text{max}}$ and $P_{\text{dc},j}^{\text{ini}}$ respectively denote the upper limit and the power before modulation of the j th DC. The amount of pumps that can be cut at each pumping and storage power station constitutes a discrete value set $\{0, P_{\text{ps},k}^1, \dots, P_{\text{ps},k}^{N_{\text{ps},k}}\}$, where $P_{\text{ps},k}^m$ denotes the amount of pumps that can be cut at the k th pumping and storage power station corresponding to the removal of m pumping and storage units, and $N_{\text{ps},k}$ is the number of units at the k th pumping and storage power station.

Equation (3) is a mixed integer nonlinear optimization problem with both discrete and continuous variables, which needs to be solved by an iterative algorithm. The optimization takes into account the dynamic safety of the system, and in each iteration needs to solve the dynamic safety index based on time domain simulation. If the initial value is not selected properly, the number of iterations is too many to complete the optimization in a short looking time. Reasonable selection of initial value is the key to reduce the number of iterations and speed up online optimization.

2.2. Two-stage Optimization Framework

In order to select reasonable initial values to speed up online optimization and ensure the rapidity of online optimization, this paper proposes a two-stage scheme optimization strategy composed of "pre-optimization" and "online optimization". Firstly, the forward-looking time T_1 and T_2 are first set, $T_1 > T_2$. In the T_1 pre-optimization stage, typical future scenarios are generated based on the prediction of future new energy and load, the corresponding control scheme is solved. Operation mode information of scenarios and control schemes are paired and stored in the optimization decision knowledge base. In the T_2 online optimization stage, accurate information about actual operation modes is obtained. The appropriate scheme in the knowledge base is selected as the initial value, and the optimization scheme under the actual operation mode is obtained by iterative optimization. The flow chart of the

optimization strategy for the two-stage scheme is shown in Figure 1.

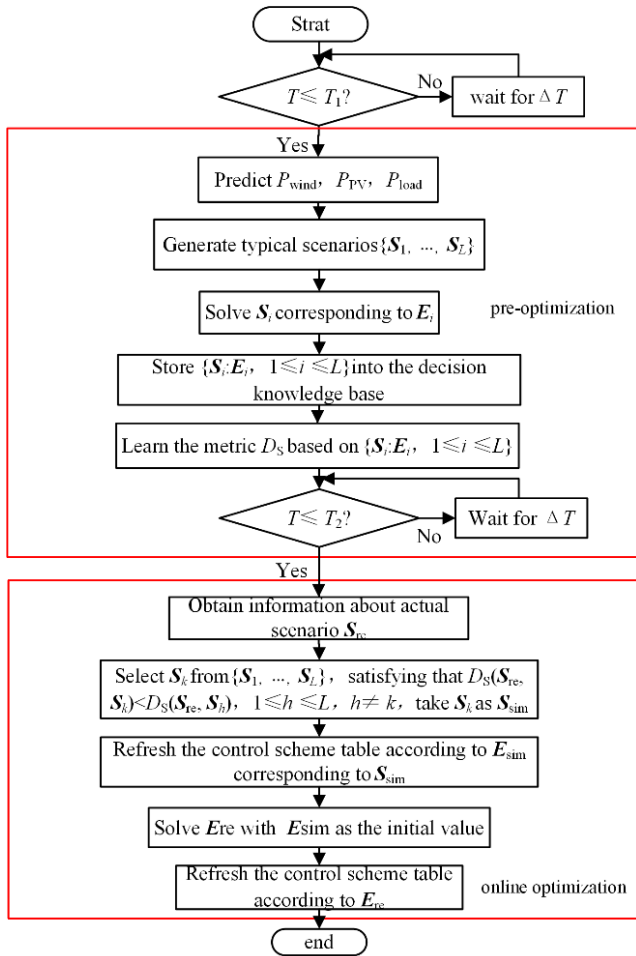


Figure 1. Rolling optimization framework of multi-resource coordinated emergency control scheme.

where T denotes time difference between the present moment and the next scheme refreshing moment, ΔT denotes the set time interval.

2.3. Pre-optimization Stage

The frequency of serious power disturbances such as DC blocking is extremely low in the actual operation of the power system, and it's difficult to collect enough scenario information from the historical operation data of the power system to generate training samples. It's necessary to construct a set of power system operation scenarios in the offline stage to simulate the frequency dynamics after power disturbances in the time domain, so as to obtain the frequency security indexes such as the maximum frequency deviation of the system under the corresponding scenarios. And then training samples for the training of the frequency security assessment model are generated. Currently, the training sample generation method usually adopts the

method of randomly varying the system operating states such as load level and new energy output within a certain range, so as to generate a batch of operating scenarios to construct the training sample set [18]. This training sample generation method is difficult to cover the actual operation of the power system, and cannot guarantee the ability of the frequency security assessment model to generalise to the future scenarios to be assessed. And it will generate a large number of training samples that are far away from the actual operation of the system, resulting in low efficiency of model training.

Generative Adversarial Network (GAN) [19], as a data-driven sample distribution learning method, can learn the sample distribution law without assuming the sample distribution function. In this paper, based on the information of the historical operation mode of the power system, we use the improved Wasserstein Distance Metric-based Generative Adversarial Network (Wasserstein Generative Adversarial Network, WGAN) to learn the distribution law of the actual operation scenario of the system. Then a batch of scenarios in line with the actual operation of the system is generated for time-domain simulation to obtain the frequency security index after the predicted power perturbation event, which is used to construct the training sample set.

2.4. Online Optimization Stage

In the online optimization stage, the time domain simulation method is applied to obtain the dynamic safety index values for scheme optimization. In order to accelerate the iteration speed of scheme optimization, the number of iterations is reduced to ensure that there is sufficient time for time domain simulation in each iteration. From $\{E_i, 1 \leq i \leq L\}$, the scheme E_{sim} that is most similar to the optimal control scheme E_{act} under the actual operation mode is selected. With E_{sim} as the initial value, the scheme is optimized online.

It's difficult to directly select E_{sim} . Therefore, E_{sim} is not directly selected in this paper. Firstly, the scenario similarity measure D_s is defined to ensure that similar scenarios correspond to similar schemes with the D_s measure. Based on D_s , the most similar scheme S_{sim} is selected from $\{S_i^f, 1 \leq i \leq L\}$. Then the corresponding scheme in the set $\{S_i^f : E_i^f, 1 \leq i \leq L\}$ is taken as E_{sim} . The initial value selection of scheme optimization which is difficult to solve directly is transformed into a similar scenario selection problem which is easy to solve. Reasonable initial value selection can significantly reduce the number of iterations of online optimization. In each iteration there is sufficient time to obtain accurate safety indicators based on time domain simulation to ensure the adaptability of the obtained scheme to the actual operation mode.

3. Solving of Multi-resource Coordinated Emergency Control Scheme

3.1. Iterative Optimization of Control Scheme Based on Trajectory Sensitivity

The optimization problem solved in the pre-optimization and online optimization stage is a nonlinear mixed integer programming problem involving dynamic safety indexes, which is difficult to be solved directly. In this paper, trajectory sensitivity method in [4] is used to locally linearize dynamic safety constraints, which are transformed into mixed integer linear programming problems for iterative solution. Local linearization and mixed integer linear programming are continuously solved, and the optimal solution is gradually approached. The iteration process is shown in Figure 2, where b denotes the counting variable, representing the b th iteration.

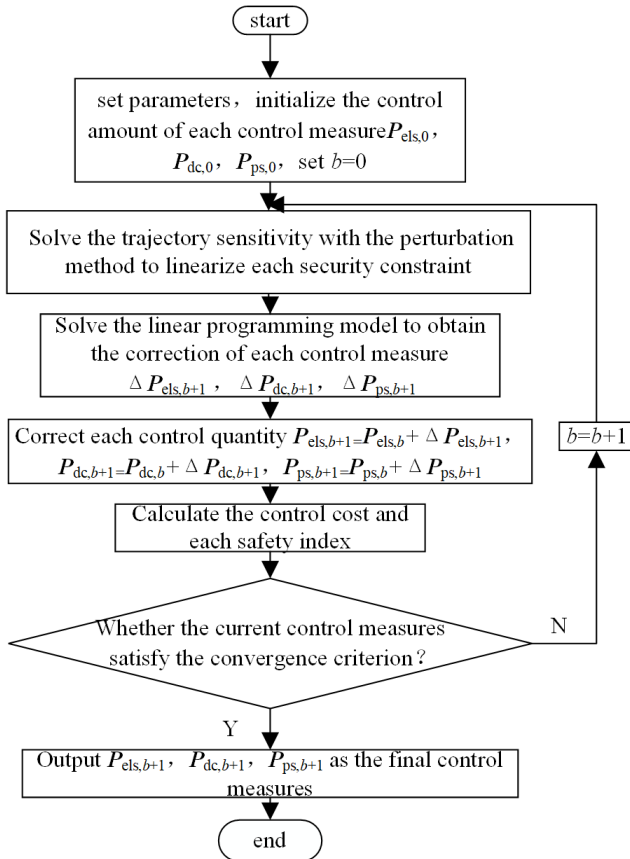


Figure 2. Rolling optimization framework of multi-resource coordinated emergency control scheme.

Where $P_{els,b}$, $P_{dc,b}$, $P_{ps,b}$ denotes the control quantity of the control measure after the b th optimization, $\Delta P_{els,b+1}$, $\Delta P_{dc,b+1}$, $\Delta P_{ps,b+1}$ denotes the correction at the $(b+1)$ th iteration.

$\Delta P_{els,b+1}$, $\Delta P_{dc,b+1}$, $\Delta P_{ps,b+1}$ are obtained by solving the mixed integer linear programming problem in the Eq. (5):

$$\begin{aligned}
 \min F(P_{els,b} + \Delta P_{els,b+1}, P_{dc,b} + \Delta P_{dc,b+1}, P_{ps,b} + \Delta P_{ps,b+1}) = \\
 \omega_{els} \sum_{i=1}^{N_{els}} (P_{els,b}^i + \Delta P_{els,b+1}^i) + \omega_{dc} \sum_{j=1}^{N_{dc}} (P_{dc,b}^j + \Delta P_{dc,b+1}^j) + \sum_{k=1}^{N_{ps}} (P_{ps,b}^k + \Delta P_{ps,b+1}^k) \\
 \text{s.t. } \eta_p^{\text{fre}}(P_{els,b}, P_{dc,b}, P_{ps,b}) + A_{els}^{\eta_p^{\text{fre}}} \Delta P_{els,b+1} + A_{dc}^{\eta_p^{\text{fre}}} \Delta P_{dc,b+1} + A_{ps}^{\eta_p^{\text{fre}}} \Delta P_{ps,b+1} > \varepsilon_{\text{fre}} \\
 p = 1, \dots, N_{\text{UPFC}} \\
 \eta_q^{\text{vol}}(P_{els,b}, P_{dc,b}, P_{ps,b}) + A_{els}^{\eta_q^{\text{vol}}} \Delta P_{els,b+1} + A_{dc}^{\eta_q^{\text{vol}}} \Delta P_{dc,b+1} + A_{ps}^{\eta_q^{\text{vol}}} \Delta P_{ps,b+1} > \varepsilon_{\text{vol}} \quad (5) \\
 q = 1, \dots, N_{\text{ref}} \\
 P_{els,b}^i + \Delta P_{els,b+1}^i \in \{0, P_{els,i}^1, \dots, P_{els,i}^{N_{els,i}}\} \\
 0 \leq P_{dc,b}^j + \Delta P_{dc,b+1}^j + P_{dc,j}^{\text{ini}} \leq P_{dc,j}^{\text{max}} \\
 P_{ps,b}^k + \Delta P_{ps,b+1}^k \in \{0, P_{ps,k}^1, \dots, P_{ps,k}^{N_{ps,k}}\}
 \end{aligned}$$

Where $A_{els}^{\eta_p^{\text{fre}}}$, $A_{dc}^{\eta_p^{\text{fre}}}$ and $A_{ps}^{\eta_p^{\text{fre}}}$ respectively denotes the sensitivity vector composed of the sensitivity of the safety index η_p^{fre} to loads shed at each load control sub-station, power modulation of each DC, and pump shedding of pumped storage at each pumping and storage power station, $A_{els}^{\eta_q^{\text{vol}}}$, $A_{dc}^{\eta_q^{\text{vol}}}$ and $A_{ps}^{\eta_q^{\text{vol}}}$ respectively denotes the sensitivity vector composed of the sensitivity of the safety index η_q^{vol} to loads shed at each load control sub-station, power modulation of each DC, and pump shedding of pumped storage at each pumping and storage power station.

According to the convergence criterion in reference [5], the iterative convergence criterion for optimization of control strategy is that the change of objective function is less than the threshold value ΔF :

$$|F(P_{els,b+1}, P_{dc,b+1}, P_{ps,b+1}) - F(P_{els,b}, P_{dc,b}, P_{ps,b})| \leq \Delta F \quad (6)$$

Or at least one of the safety indicators satisfies the critical value, that is, at least one of the Eq. (7) satisfies:

$$\begin{aligned}
 0 < \eta_p^{\text{fre}}(P_{els,b+1}, P_{dc,b+1}, P_{ps,b+1}) - \varepsilon_{\text{fre}} < \Delta \varepsilon_{\text{fre}} \\
 p = 1, \dots, N_{\text{UPFC}} \\
 0 < \eta_q^{\text{vol}}(P_{els,b+1}, P_{dc,b+1}, P_{ps,b+1}) - \varepsilon_{\text{vol}} < \Delta \varepsilon_{\text{vol}} \quad (7) \\
 q = 1, \dots, N_{\text{ref}}
 \end{aligned}$$

Where $\Delta \varepsilon_{\text{fre}}$, $\Delta \varepsilon_{\text{vol}}$ denotes the specified convergence threshold, set to a small positive number.

Through the above trajectory sensitivity method, the mixed integer nonlinear programming problem in the pre-optimization and online optimization stage can be transformed into the mixed integer linear programming problem as shown in the equation (5), so that the mature Benders decomposition method can be further solved [20].

3.2. Control Measure Sensitivity Solution

The key to local linearization is to solve the trajectory sensi-

tivity vector. Because of the high dimensional nonlinearity of power system, it is difficult to use analytical method to directly solve the trajectory sensitivity. In this paper, based on perturbation method, the trajectory sensitivity is solved:

$$a_x^y = \frac{y(x^k + \Delta x) - y(x^k)}{\Delta x} \quad (8)$$

Where a_x^y denotes the sensitivity of safety index y to the control quantity x of a control measure, y can be set η_p^{fre} or η_q^{vol} , x can be the load shed at a load control sub-station, power modulation of a DC, or the cutting pump quantity of a pumping and storage power station, x^k is the value of the control quantity at the k th iteration, Δx is the momentum, $y(x^k)$ denotes the value of safety index y with the control quantity x^k .

In the pre-optimization stage, multiple iterations of the optimization scheme for a large number of scenarios are carried out. If $y(x^k)$ is obtained based on time domain simulation in each iteration to calculate the trajectory sensitivity, the calculation time is long, and it's difficult to ensure that the pre-optimization can be completed within the specified forward-looking time. Therefore, in the pre-optimization stage of this paper, the machine learning model for evaluating $y(x^k)$ is constructed based on the method described in [21] to reduce the pre-optimization time and ensure that it's completed within the specified forward-looking time.

In the online optimization stage, accurate information about actual operation modes can be obtained. The control scheme can be optimized aiming at the determined scenario. In order to ensure the adaptability of the scheme to the actual operation scenario, the accurate value of $y(x^k)$ should be obtained based on the time domain simulation to calculate the sensitivity of the measure. In order to ensure the decision-making efficiency of the control scheme, it is necessary to reasonably select the initial optimization value of the scheme. The relevant content is shown in Section 3.

4. Selection of the Initial Value in the Online Optimization Stage

4.1. Scenario Similarity Measurement

For control schemes E_i and E_j , similarity is measured by Euclidean distance between them, and $D_E(E_i, E_j)$ in Section 1 is defined as follows:

$$D_E(E_i, E_j) = \|E_i - E_j\|_2 = \sqrt{\sum_{k=1}^M (P_k^i - P_k^j)^2} \quad (9)$$

In the online optimization stage, accurate information about the actual operating scenario S_{act} characterized by

steady-state power flow features can be obtained. In this paper, scenario similarity measure D_S to ensure that $D_E(E_i, E_j) < D_E(E_i, E_k)$ if $D_S(S_i, S_j) < D_S(S_i, S_k)$, where $1 \leq i, j, k \leq L$, and i, j , and k are not equal. From $\{S_i, 1 \leq i \leq L\}$, S_j is selected to satisfy that for any k , $1 \leq k \leq L$, $k \neq j$, and $D_E(E_{\text{act}}, E_j) < D_E(E_{\text{act}}, E_k)$ if $D_S(S_{\text{act}}, S_j) < D_S(S_{\text{act}}, S_k)$. Then the scheme S_j corresponding to E_j is selected to be E_{sim} . In this way, the initial value of optimization iteration of suitable scheme is obtained. The scene similarity measure D_S is learned from the decision knowledge base $\{S_i; E_i, 1 \leq i \leq L\}$.

According to the metric D_S , similarity between S_i and S_j $D_S(S_i, S_j)$ can be calculated to reflect the similarity between different scenarios. Similarly to Eq. (10), D_S is defined as follows:

$$D_S(S_i, S_j) = \sqrt{\sum_{k=1}^N (p_k^i - p_k^j)^2} \quad (10)$$

If D_S is directly applied in the equation (8), it's difficult to ensure that the corresponding control schemes of similar scenarios are similar. Therefore, in this paper, the metric transformation matrix T is introduced, which is equivalent to the scene similarity measure changing from D_S to D_S^T as follows:

$$D_S^T(S_i, S_j) = D_S(TS_i, TS_j) \quad (11)$$

4.2. Scenario Similarity Measurement Learning

The key of metric learning lies in the solution of metric transformation matrix T . The transformation from S_i to TS_i with the metric matrix T satisfies that for any unequal i, j, k , Eq. (12) satisfies:

$$\begin{aligned} & [D_S^T(S_i, S_j) - D_S^T(S_i, S_k)] \times \\ & [D_E(E_i, E_j) - D_E(E_i, E_k)] > 0 \end{aligned} \quad (12)$$

$1 \leq i, j, k \leq L$

In this paper, U in Eq. (13) is used as the loss function, and the gradient descent method is used to solve the transformation matrix T :

$$\begin{aligned} \arg \min U(T) = \\ \sum_{i=1}^L \sum_{j=1}^L \sum_{k=1}^L \text{sign}[(D_S^{T,ij} - D_S^{T,ik})(D_E^{ik} - D_E^{ij})] \end{aligned} \quad (13)$$

$j \neq i, k \neq i, j$

Where $\arg \min U(T)$ represents the parameter T that takes the minimum loss function $U(T)$, $D_S^{T,ij}$ represents $D_S^T(S_i, S_j)$, $D_S^{T,ik}$ represents $D_S^T(S_i, S_k)$, D_E^{ik} represents $D_E(E_i, E_k)$, D_E^{ij} represents $D_E(E_i, E_j)$, and $\text{sign}(\bullet)$ represents the symbolic function.

The goal of minimizing the loss function in Eq. (14) is to

ensure that for scenarios S_i, S_j, S_k and their corresponding control schemes E_i, E_j, E_k , the equation (14) is satisfied:

$$(D_S^{T,ij} - D_S^{T,ik})(D_E^{ik} - D_E^{ij}) > 0 \quad (14)$$

Where λ represents the regularization coefficient and $\lambda > 0$.

The optimization problem in Eq. (13) is solved as shown in Table 1.

Table 1. Solving process of the optimization problem.

Solving process of the optimization problem

Step 1 set $q=1$, select the scenario S_i and the corresponding scheme E_i

Step 2 select the scenario S_j and S_k , satisfying that $D_E^{ij} < D_E^{ik} < D_E^{ih}, (D_S^{T,ij} - D_S^{T,ik})(D_E^{ij} - D_E^{ik}) \neq 0$

Step 3 calculate $(\frac{\partial Q}{\partial T S_i}, \frac{\partial Q}{\partial T S_j}, \frac{\partial Q}{\partial T S_k})$ to update T , set $q=q+1$

Step 4 repeat the above iterative process, until $\max(|\alpha_{mn}^{q+1} - \alpha_{mn}^q|) < \varepsilon$ and $|Q^{q+1} - Q^q| < \mu, 1 \leq m \leq N, 1 \leq n \leq N$,

5. Case Study

The simplified provincial power grid in literature [21] is used as a numerical example to verify the effectiveness of the proposed method, including about 150 buses and 80 lines. The geographical wiring diagram of the power grid for example is shown in Figure 3. The base load of the system is 58 GW, and DC #2 with 8 GW power feed in is taken as the disturbance event. DC #1 with 4 GW power and DC #3 with 8 GW power are taken as the controlled DC.

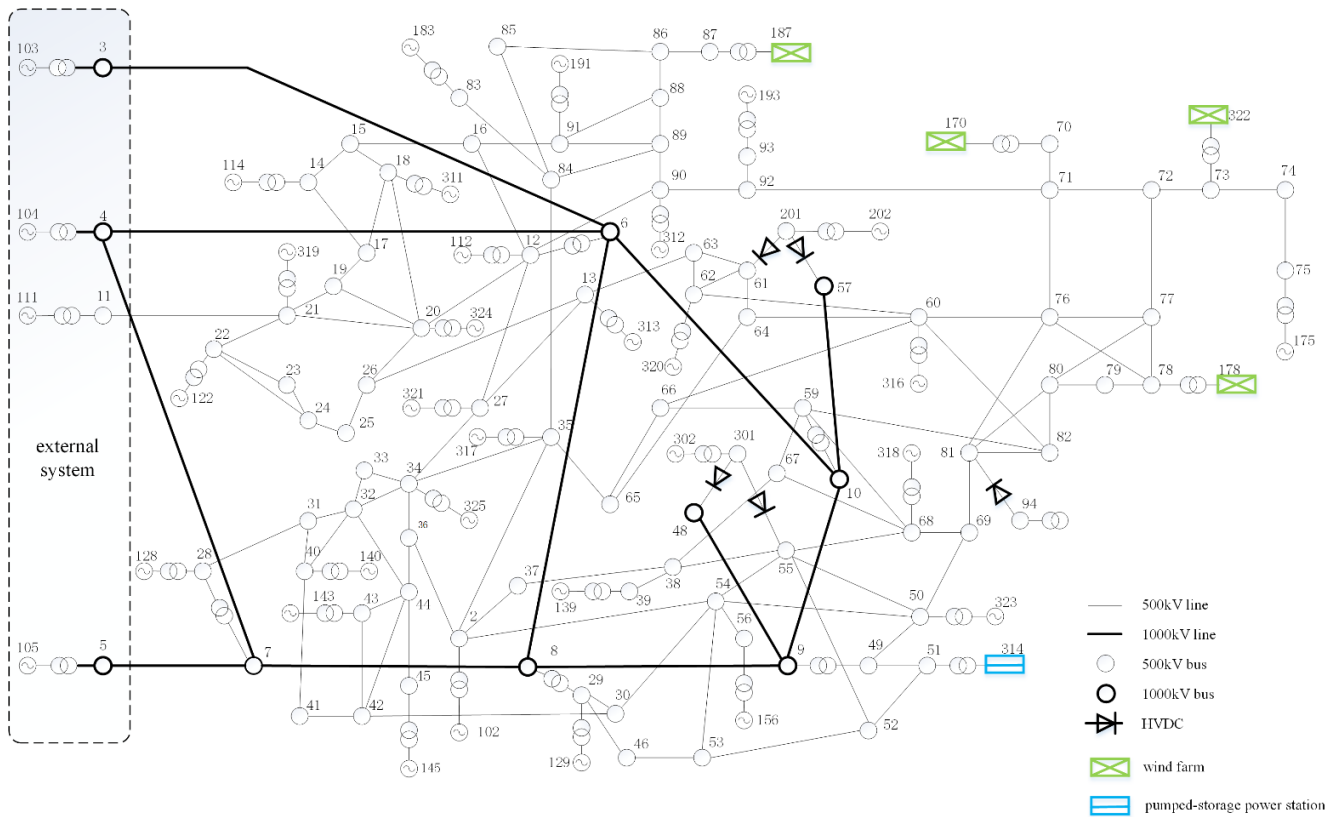


Figure 3. Example grid geographic wiring diagram.

5.1. Evaluation and Validation of Dynamic Security Indicators Based on Machine Learning

The pre-optimization stage is to quickly solve the optimal control scheme in a large number of scenarios, and use the machine learning method to quickly evaluate the dynamic safety indicators. It's necessary to train the relevant machine learning model in advance, and then solve the multi-resource coordination emergency control optimization scheme based on the method in Section 2. The wind power data used in this paper are 1 month wind power data of 170, 178, 187, 322 nodes of the system and 1 month load data of each load node. Every 10 min is a time section, and there are 4464 time sections in total. In this

paper, the prospective time $T_2=10$ mi, $T_1=1$ h.

12 continuous time sections are randomly selected as the refreshing period of the control scheme, and the remaining 4452 time sections are regarded historical data to predict future typical scenarios and generate training and testing samples of the machine learning evaluation model. Based on historical data, 4452 samples are obtained by time domain simulation, 80% as training samples and 20% as test samples. The training and test errors of the obtained machine learning evaluation model are shown in Table 2. Frequency and voltage security indicators training error root mean square, maximum training error, test error root mean square, maximum test error are shown in Table 2.

Table 2. Training and test error of machine learning model.

frequency security indicator	$\epsilon_{\max}^{\text{train}}$	$\epsilon_{\text{rmse}}^{\text{train}}$	$\epsilon_{\max}^{\text{test}}$	$\epsilon_{\text{rmse}}^{\text{test}}$
η^{fre}	0.0003	0.00023	0.0007	0.00035
η^{vol}	0.0002	0.00016	0.00076	0.0005

It can be seen from Table 2 that with the constructed machine learning evaluation model, the evaluation error of the constructed machine learning evaluation model for frequency and voltage safety is small and within the allowable range.

5.2. Validation of Optimization Accuracy of Control Scheme at Pre-learning Stage

L is set 200 in Section 1, and the scenario generation method in Reference [21] is used to generate 200 typical future scenarios. The method in Section 2 is used to solve the control scheme under each scenario, and the scenario information and corresponding control scheme are stored in the knowledge base. Iterations, values of security indicators and costs of schemes are shown in Table 3. In this example, margin of voltage security indicators is large, and the dominant security factor is frequency security indicator η^{fre} . Therefore, only η^{fre} is shown here.

As shown in Table 3, with the method proposed in this paper, cost of control schemes can be reduced while the se-

curity indicators satisfying the requirements. The comparison between the optimization control solution of trajectory sensitivity calculated based on machine learning model and trajectory sensitivity calculated using time-domain simulation method is shown in Table 4, where P_{total} represents the control quantity, t_{cal} represents the calculation time.

Table 3. Values of each index in the iteration process.

N_{Tra}	N_{Bend}	$\eta_{\text{ml}}^{\text{fre}}$	$\eta_{\text{real}}^{\text{fre}}$	F
0	\	-0.11313	-0.11352	0
1	7	0.08523	0.08576	381.1
2	9	0.02134	0.02154	365.2
3	13	0.00751	0.00731	321.6
4	6	0.00103	0.00128	313.2

Table 4. Comparison between machine learning and time domain simulation methods for trajectory sensitivity.

evaluation method	P_{total}	t_{cal}	F	η^{fre}
machine learnig	5.61 GW	12.5 s	313.2	0.00128
time-domain simulation	5.49 GW	3818.2 s	297.4	0.00101

The time for calculating the dynamic security indicators with time-domain simulation method is about 214.6 h, which is much longer than 1 h prospective time. By using the machine learning method to calculate the dynamic security indicators, the total time required to solve the control scheme under 200 scenarios is only 27.3 min within the 1 h forward-looking period.

5.3. Comparison of Optimization Process Under Different Initial Values in Online Optimization Stage

When entering the forward-looking period of 10 min, it's necessary to match the scene that is most similar to the actual

operation mode as the initial value, and iteratively optimize to obtain the optimal control scheme. λ is set 0.1, ε and μ are respectively set 0.075 and 300. The training process converges after about 32 generations, and the training time is only 141.2 s. The similarity between the future scene and the actual scene is measured based on D_S^T , and the most similar scene obtained by using D_S^T measurement is the 119th scene.

P_{total} , t_{cal} , N_{Tra} , N_{Ben} , F and η^{fre} obtained based on different measurement are shown in Table 5, where N_{sce} represents the selected scenario number. Ten random initial values are selected to optimize the scheme, and the average value of each initial value is compared with the optimized scheme obtained in this paper.

Table 5. Comparison of optimization results under different initial value selection schemes.

selection method	N_{sce}	$P_{\text{total}}/\text{GW}$	N_{Tra}	N_{Ben}	t_{cal}/s	F	$\eta^{\text{fre}}/\times 10^{-3}$
random	/	5.41	8	45	2303	288	1.02
D_S	34	5.42	5	22	1089	289	1.03
D_S^T	119	5.41	2	3	136	287	1.02

As shown in Table 5, compared with D_S , with the measurement proposed in this paper a better initial value can be provided for the iterative optimization of the control scheme in the actual operation mode. The number of optimization iterations can be reduced, ensuring that the online optimization of the control scheme can be completed within 10 min foresight time.

5.4. Comparison with Other Methods

The optimization method of emergency control scheme in this paper is further compared with the Random Forest (RF) model in literature [22] and the Convolutional Neural Network in [23], as shown in Table 6.

Table 6. Comparison of optimization results with different optimization methods for emergency control schemes.

frequency security indicator	the two-stage optimization method	RF	CNN
P_{total}	5.41 GW	7.27 GW	5.02 GW
t_{cal}	136.7 s	3.2 s	2.1 s
F	287.6	389.9	221.8
η^{fre}	0.00102	0.00278	0.00089

Compared with the other two methods, in the two-stage optimization method proposed in this paper, time domain simulation is used to solve the corresponding security indicators in the online optimization stage, which ensures the accuracy of the calculation results. In the final optimal control scheme, the system safety index η^{fre} is 0.00102, which meets the corresponding requirements, and the control cost of the obtained control scheme is small. At the same time, the initial values

are provided for the online optimization stage at the pre-optimization stage, which improves the optimization efficiency and reduces the optimization time. Although the final optimization time is 136.7 s, which is higher than 3.2 s of the RF method and 2.1 s of the CNN method, it's still far less than the stipulated prospect time of 10 min in the online optimization stage, ensuring that the scheme optimization can be completed within the stipulated 10 min prospect time.

6. Conclusions

In this paper, a two-stage optimization strategy of pre-optimization and online optimization is proposed to optimize the emergency control scheme of multi-DC power grid with large-scale new energy. The machine learning method is used in the pre-optimization stage, therefore the dynamic security indicators can be quickly assessed after the corresponding control measures are adopted in typical future scenarios. Through taking the appropriate scheme in the decision knowledge base constructed in the pre-optimization stage as the initial value of iterative optimization, the optimization process of emergency control scheme in the online optimization stage can converge quickly. Thus, there is enough time to calculate the accurate value of dynamic security indicators based on the time-domain simulation method, and the adaptability of the emergency control scheme to the actual operation scenario is improved. The simulation example shows that with the proposed method, cost of the control scheme is reduced while security indicators satisfy the requirements. Based on the research content of this paper, further research about the optimization method of control measures considering multiple safety attributes such as frequency and voltage at the same time can be done.

Abbreviations

HVDC	High Voltage Direct Current
UFLS	Under Frequency Load Shedding
GAN	Generative Adversarial Network
WGAN	Wasserstein Generative Adversarial Network

Author Contributions

Li Huarui: Conceptualization, Data curation, Formal Analysis, Methodology

Zhu Xinyao: Methodology

Acknowledgments

The authors would like to thank the financial support by National Key Research and Development Plan of China (2024YFB2408900).

Conflicts of Interest

The authors declare no conflicts of interest.

References

- [1] HONG Hanxiao, WU Chenxi, NI Suoyin. Optimal scheduling of new-type power system considering frequency-inertia security constraints [J/OL]. *Electric Power Automation Equipment*: 1-12 [2024-07-01]. <https://doi.org/10.16081/j.epae.202312046>
- [2] LIN Hengxian, HOU Kaiyuan, CHEN Lei, et al. Unit commitment of high-proportion of wind power system considering frequency safety constraints [J]. *Power System Technology*, 2021, 45(1): 1-9. <https://doi.org/10.13335/j.1000-3673.pst.2020.0190a>
- [3] LUO Yazhou, CHEN Dezhi, LI Yiqun, et al. Design of system protection scheme for North China multi-UHV AC and DC strong coupling large receiving-end power grid [J]. *Automation of Electric Power Systems*, 2018, 42(22): 11-18. <https://doi.org/10.7500/AEPS20180529008>
- [4] CAO Yongji, ZHANG Hengxu, XIE Yuzheng, et al. Configuration scheme of emergency load shedding for HVDC receiving-end power grid based on transient low-frequency and high-voltage features [J]. *Automation of Electric Power Systems*, 2019, 43(6): 156-164. <https://doi.org/10.7500/AEPS20180404006>
- [5] XU Xin, ZHANG Hengxu, LI Changgang, et al. Emergency load shedding optimization algorithm based on trajectory sensitivity [J]. *Automation of Electric Power Systems*, 2016, 40(18): 143-148. <https://doi.org/10.7500/AEPS20151116002>
- [6] SUN Dayan, ZHOU Haiqiang, XIONG Haoqing, et al. Sensitivity analysis based emergency load shedding optimization method for the HVDC receiving end system [J]. *Proceedings of the CSEE*, 2018, 38(24): 7267-7275+7453. <https://doi.org/10.13334/j.0258-8013.pcsee.180127>
- [7] ZHAO Jinquan, TANG Jianjun, WU Di, et al. Emergency coordination control strategy for transient voltage and transient frequency stability in HVDC infeed receiving-end power grid [J]. *Automation of Electric Power Systems*, 2020, 44(22): 45-53. <https://doi.org/10.7500/AEPS20191019002>
- [8] YUAN Sen, CHEN Dezhi, LUO Yazhou. Stability characteristics and coordinated control measures of multi-resource for DC blocking fault impacting weak AC channel [J]. *Electric Power Automation Equipment*, 2018, 38(8): 203-210. <https://doi.org/10.16081/j.issn.1006-6047.2018.08.029>
- [9] LI Zhaowei, FANG Yongjie, HUANG Hui, et al. Coordinated control of cross-region DC frequency control and emergency power support in system protection [J]. *Automation of Electric Power Systems*, 2020, 44(22): 31-36. <https://doi.org/10.7500/AEPS20200114014>
- [10] BAO Yanhong, FENG Changyou, XU Taishan, et al. Online security and stability comprehensive auxiliary decision making of power system [J]. *Automation of Electric Power Systems*, 2015, 39(1): 104-110. <https://doi.org/10.7500/AEPS20141017001>
- [11] WANG Zengping, ZHU Shaoxuan, WANG Tong, et al. Research on stratified optimal load shedding strategy for receiving end power grid [J]. *Transactions of China electrotechnical society*, 2020, 35(5): 1128-1139. <https://doi.org/10.19595/j.cnki.1000-6753.tces.190377>
- [12] WANG Changjiang, LI Xiaojing, JIA Chunhe, et al. Trajectory sensitivity based transient voltage two-stage control in AC / DC receiving end system [J]. *Electric Power Automation Equipment*, 2023, 43(07): 124-132. <https://doi.org/10.16081/j.epae.202212023>

- [13] ZHANG Zhe, QIN Boyu, GAO Xin, et al. Emergency control strategy of power grid voltage stability based on convolutional neural network and long short-term memory network [J]. *Automation of Electric Power Systems*, 2023, 47(11): 60-68. <https://doi.org/10.7500/AEPS20220712005>
- [14] GUO Ting, XIE Min, LIU Mingbo. Reduced space algorithm for model predictive transient voltage stability emergency control [J]. *Proceedings of the CSEE*, 2012, 32(16): 53-61. <https://doi.org/10.13334/j.0258-8013.pcsee.2012.16.008>
- [15] BI Zhaodong, WANG Jianquan, HAN Zhenxiang. A fast load shedding algorithm based on integral sensitivity [J]. *Power System Technology*, 2002, 26(8): 4-7. <https://doi.org/10.13335/j.1000-3673.pst.2002.08.002>
- [16] CHEN Qing, ZHOU Haiqiang, ZHU Bin, et al. Coordinated emergency load shedding control optimization algorithm [J]. *Power System Technology*, 2016, 40(4): 1044-1050. <https://doi.org/10.13335/j.1000-3673.pst.2016.04.010>
- [17] WANG Tong, LIU Jiuliang, ZHU Shaoxuan, et al. Transient stability assessment and emergency control strategy based on random forest in power system [J]. *Power System Technology*, 2020, 44(12): 4694-4701. <https://doi.org/10.13335/j.1000-3673.pst.2019.0909>
- [18] ZHANG Hengxu, LI Changgang, LIU Yutian. Quantitative frequency security assessment method considering cumulative effect and its applications in frequency control [J]. *International Journal of Electrical Power & Energy Systems*, 2015, 65(65): 12-20. <https://doi.org/10.1016/j.ijepes.2014.09.027>
- [19] CAO Yongji, ZHANG Hengxu, ZHANG Yi., et al. Event-driven fast frequency response control method for generator unit [J]. *Automation of Electric Power Systems*, 2021, 45(19): 148-154. <https://doi.org/10.7500/AEPS20210210001>
- [20] TIAN Xichen, GUO Hongye, LI Kexin, et al. Power source planning method satisfying unit cost recovery constraints under market environment [J]. *Electric Power Automation Equipment*, 2023, 43(05): 252-258. <https://doi.org/10.16081/j.epae.202303030>
- [21] LI Huarui, LI Changgang, LIU Yutian. Machine learning-based frequency security early warning considering uncertainty of renewable generation [J]. *International Journal of Electrical Power & Energy Systems*, 2022, 134. <https://doi.org/10.1016/j.ijepes.2021.107403>
- [22] FU Junpeng, CHEN Xiuhong, GE Xiaoqian. Uncorrelated linear discriminant analysis with L2,1-norm regulation and its application in face recognition [J]. *Computer Engineering & Science*, 2017, 39(02): 343-350. <https://doi.org/10.3969/j.issn.1007-130X.2017.02.019>
- [23] CAO Zhen, ZHUANG Jun, XUE Jinhua, et al. Optimization of emergency control strategy for frequency of receiving-end power grid under DC blocking based on improved particle swarm optimization and hybrid convolutional neural network [J/OL]. *Modern Electric Power*: 1-12. [2024-02-01]. <https://doi.org/10.19725/j.cnki.1007-2322.2023.0132>

Research Field

Li:Huarui frequency security of power system, voltage security of power system, economic dispatching of power system, planning and Operation of power system, dynamic simulation of power system

Zhu Xinyao: frequency security of power system, voltage security of power system, economic dispatching of power system, planning and Operation of power system, dynamic simulation of power system